

NIP ROLLER INDUCED CONTACT STRESSES

By

CHUNBAO XU

Bachelor of Science

Beijing University

Beijing, China

1988

Submitted to the Faculty of the
Graduate College of the
Oklahoma State University
in partial fulfillment of
the requirements for
the Degree of
MASTER OF SCIENCE
May, 1995

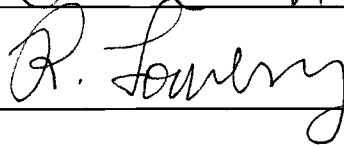
NIP ROLLER INDUCED CONTACT STRESSES

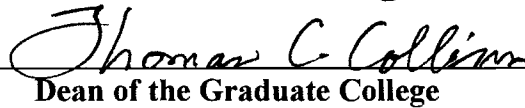
Thesis Approved:



Thesis Adviser







Dean of the Graduate College

ACKNOWLEDGMENTS

I wish to express my sincere appreciation to my graduate advisor, Dr. J. K. Good, for his tremendous support, guidance and assistance throughout this research project. I also wish to thank my other committee members, Dr. R. L. Lowery and Dr. C. E. Price, for sacrificing their time. My thanks also go to Dr. T. Minahen for his counsel at the beginning of this project.

I extend thanks to the Web Handling Research Center for providing this research opportunity. And thanks go to graduate students Will, Yunpeng and Nanda for their help and friendship.

Finally, I give my gratitude and appreciation to my sister Xiao and to my parents, Fengchuan and Shouren, for their sacrifices and support. I also give sincere gratitude to my American parents, Ray and Louise, who gave me so much love and supported me all the way.

TABLE OF CONTENTS

Chapter	Page
I. INTRODUCTION.....	1
II. LITERATURE REVIEW.....	3
III. CONTACT OF ELASTOMERIC COVERED ROLLER WITH RIGID ROLLERS.....	9
Experimental Setup.....	9
Tekscan Measurement.....	11
Hertz's Theory.....	13
Finite Element Analysis.....	16
Comparison of Results.....	18
Mooney-Rivlin Materials	23
IV. CONTACT OF A RIGID ROLL WITH A WINDING ROLL.....	27
Experimental Setup.....	27
Material Properties of Bond Paper.....	28
Pull-Tabs Calibration.....	30
Hakiel's Model.....	31
Finite Element Analysis.....	33
V. CONCLUSIONS AND FUTURE WORK.....	38
Conclusions.....	38
Future Work.....	39
REFERENCES.....	40

LIST OF TABLES

Table	Page
I. Comparision of Area Beneath Three Curves.....	23

LIST OF FIGURES

Figures	Page
1-1. Pacer or Drive Roll Geometry.....	3
1-2. A Nip in Contact with a Winding Roll Application.....	3
3-1. A Schematic Diagram of the System Experimental.....	10
3-2. Nip Loads vs. Air Pressure Applied.....	11
3.3. Contact Rollers.....	13
3-4. Variation of Maximum Pressure with Nip Load(Hard Rubber).....	15
3-5. Finite Element Grid.....	18
3-6. Variation of Contact Width with Nip Load.....	19
3-7. Variation of Maximum Pressure with Nip Load(Soft Rubber).....	20
3-8. Pressure Distribution on Contact Surface -- Nip Load = 6.6lbs/in.....	21
3-9. Pressure Distribution on Contact Surface -- Nip Load = 8.8lbs/in.....	21
3-10. Pressure Distribution on Contact Surface -- Nip Load = 20lbs/in.....	22
3-11. Correlation with a Straight Line Using the Mooney-Rivlin Constitutive Equation.....	24
3-12. Pressure Distribution on Contact Surface.....	26
3-13. Comparison of Results from FEM and Spengos.....	26
4-1. Layer of Center Winding with Nip Roller on 3M Splicer Winder.....	28

Figures	Page
4-2. Pull Tab Calibration.....	31
4-3. Interlayer Pressures Distribution.....	32
4-4. Pressure Distribution on Contact Surface (Wound Paper Roller).....	37

NOMENCLATURE

E	modulus of elasticity
E_1	Young's modulus of nip roller
E_2	Young's modulus of rubber
E_r	radial modulus of a wound roll
E_θ	tangential modulus of a wound roll
ν	Poisson's ratio
ν_1	Poisson's ratio of nip roller
ν_2	Poisson's ratio of rubber
R	radius of roller
N	RPM
α	angle of inner face of the rubber covering
β	angle of outer face of the rubber covering
P	nip load
$p(x)$	pressure distribution at contact area between rollers
a	half contact width at contact surface
R_c	radius of core
P_m	maximum pressure on the contact area between rollers
θ	tangential direction

p	radial pressure
h	web thickness
μ	coefficient of friction betweensheets of paper
a_{ij}	material constants of wound roll in Polar coodinates
b_{ij}	material constants of wound roll in Cartesian coodinates
$G_{r\theta}$	shear modulus at Polar coodinates

CHAPTER I

INTRODUCTION

1.1 Overview

Flexible, continuous sheet materials, called webs, are often modified in process machinery to add value to the web. Printing, coating, and laminating are examples of web processes in which value is added to the web prior to its conversion to a discrete product, such as a newspaper or possibly a wrapper for a food product. In web processing machinery, the web will come into contact with rollers called "nip rolls". The purpose of the nip roll is to provide enough traction to pull the web through the process machinery. A nip roller typically involves two rollers, one whose surface is incompressible (i.e., rubber and like materials) and one whose surface is compressible (i.e., typically a metal material).

There are two common applications of nip rollers in web lines. One application is that of a pacer or drive roller. The purpose of this type of a roller is to control the tension and velocity of the web. To prevent slippage, the web passes through two rollers which are in intimate contact, as shown in Figure 1.1. The second application of a nip roller is that of a rider or lay-on roller in contact with a winding roll. In this application the purpose of the nip roller may either be to (1) drive the winding roll or (2) to exclude air which is attempting to enter the winding roll as shown in Figure 1.2.

In either application, the web is subjected to normal contact stresses similar to those first quantitatively described by Hertz[1]. These contact stresses can either

improve or degrade web quality. In the paper industry, the paper is forced to transgress nip rollers called calendar rolls. The paper is intentionally subjected to contact and shearing stresses which result in a smoother web surface and, therefore, improved quality. In most cases, however, the contact stresses are detrimental to quality. Coating is a common web process in which value is added to the web. In sections of the web machinery near the coating operation, a nip roller can spell disaster because the coating may have higher affinity for the nip rollers than for the web. Relatively little is known concerning the absolute values of those contact stresses. Some researchers, as discussed in the literature review, have chosen to model these contact stresses through extensions of Hertz's contact relationships, which were originally derived for isotropic materials.

1.2 Purpose

The purpose of this research is to remove as many of the simplifying assumptions as possible, to study how the contact stresses behave in cases in which the roller materials are (1) incompressible or (2) have complex properties due to being composed of multiple layers of web. Both analytical and experimental investigations will be performed. The outcome of this research will aid those engineers who are responsible for transporting webs, whose quality is affected by contact stresses.

1.3 Organization

A literature survey addresses contact topics in Chapter 2. A plane strain model for rubber covered rolls in contact with rigid rolls is developed in Chapter 3. A model is developed in Chapter 4 for the contact of a nip roll with a winding roll. An additional complexity is involved in this case since the radial modulus of elasticity of the winding roll is a function of the contact pressure between web layers. In Chapter 5, the

conclusions of this research are presented, followed by possible avenues of future research.

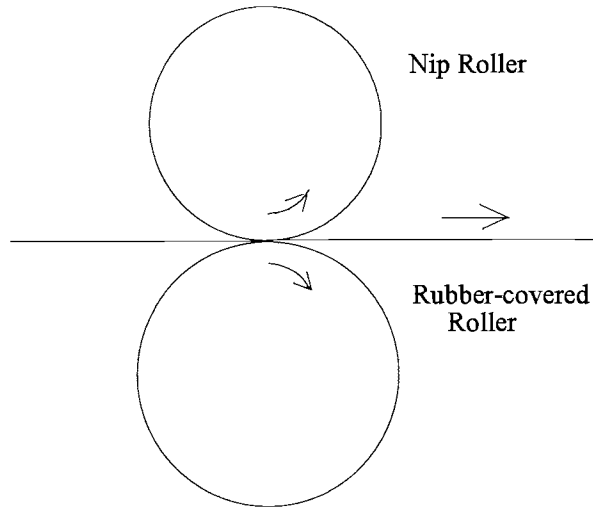


Fig. 1.1 Pacer or Drive Roll Geometry

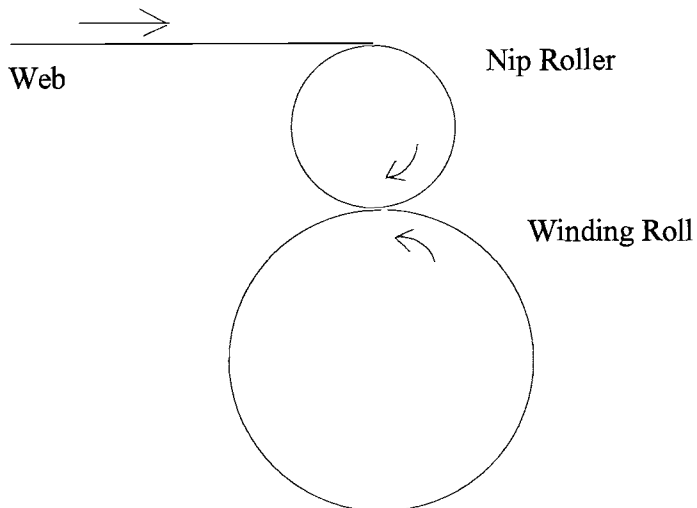


Fig. 1.2 A Nip in Contact with a Winding Roll

CHAPTER II

LITERATURE REVIEW

Hertz's contact theory of two elastic bodies was published in 1881[1]. This problem has received much attention and has been studied by several researchers. Due to the complexity of the problem and instrumentation difficulties, experimental investigations have been rather infrequent and most researchers have employed numerical techniques, typically finite element methods, to solve the problem.

In 1950, Hannah[3] modified Hertz's theory of contact for a roll which consists of a thin elastic cover on a rigid core. She studied the effects of material, thickness of the cover, the pressure between rollers and the roller size on the contact area, deformation of the cover and the contact pressure. She mathematically considered the problem as one of generalized plane stress in an elastic layer, with given displacement conditions on the interface between metal and cover, and subjected to pressure by a body of given shape on its free face.

Hannah found that, next to the roller diameter and elastic modulus, the layer thickness is the most important factor determining the relationship between loading and deformation for this type of roller. The pressure distribution over the contact zone is only slightly affected by layer thickness. However, a change in Poisson's ratio makes an appreciable difference to the loading necessary for a given contact length but has very little effect otherwise. Slipping at the inner surface gives results very similar to those with a fixed surface and a zero value of Poisson's ratio.

Parish[4], in 1955, conducted an experiment to measure the pressure distribution between two rollers in contact. He used the method of pressure distribution measurement which consisted of mounting a pressure transmitting pin in a radial hole in one of the rollers with its outer end flush with the roller surface and its inner end in contact with some pressure-sensitive device inside the roller. As the outer end of the pin passes through the nip, the variations in load are transmitted to the pressure-sensitive device where they are converted to some form which may be extracted from the roller and displayed to represent the original distribution of pressure. He compared the load per linear inch on the nip with that found from the integrated area under the pressure distribution curve and found a good agreement between them.

In 1958, Parish[5] worked out the theoretical relation between the roller load and cover tangential surface strain in the cover for Hannah's case, modified to plane strain conditions. He made the changes by replacing $\nu/(1+\nu)$ by ν and E by $E/(1-\nu^2)$ in Hannah's results. He also made an experimental investigation and compared his results with that obtained from Hannah's solution after modification for plane strain. A noticeable discrepancy was observed between his experimental pressure distribution and the theoretical distribution. Parish suggested that the probable causes of this discrepancy might have arisen from the following assumptions, none of which were satisfied exactly by the experiment:

- 1) the nip width and the cover thickness are small as compared with roller diameter,
- 2) strains are infinitesimal,
- 3) the material of the cover possesses linear elastic properties
- 4) the rollers are stationary.

But, the most likely cause of the discrepancy, as Parish pointed out, was the non-linearity in the elastic properties of the rubber.

In 1961, Parish[6] supplied an empirical method of finding the indentation under load based on his own experimental measurements. He extended his research to

conditions of uneven load distribution along the length of the rollers. Experiments were made with both stationary and rotating rollers. He found that the static nip widths are larger than dynamic ones and the difference generally lies between 5 and 10%.

Foreman[7], in 1964, investigated the speed change of a strip being processed by pinch rolls and bridles. He showed that the strip velocity through a rubber covered pinch roll could be calculated using

$$v_w = \frac{2 \pi R N \alpha}{\beta}$$

where α/β will have a value of 1.0 to 1.1, depending on the characteristics of the rubber covering and the roll pressure. This greater velocity is not due to slipping, but to the indentation of the rubber covering. The covering must speed up if indented. This is analagous to an incompressible fluid encountering a constriction in a flow channel. In the vicinity of the constriction, the velocity of the fluid must increase. He tested the accuracy of his theoretical reasoning by conducting experiments and concluded:

- 1) increasing the radius of the roll will decrease the value of the factor α/β due to a wider nip and consequently a lower net pressure,
- 2) unless the covering thickness is made quite thin, there is no benefit from reducing the thickness,
- 3) increasing the covering hardness will proportionately decrease the value of α/β , and
- 4) decreasing the roll pressure will decrease the value of α/β .

The experimental work of Spengos[8], in 1965, was quite extensive and involved a wide range of loads, thickness of the rubber layer and speed differences between the mating rollers. A steel cylinder, driving a rubber-covered cylinder, was instrumented for a quantitative, as well as qualitative, investigation of the action taking place in the contact area. Spengos found that the transmission of a tangential force through the

contact alters the radial pressure distribution considerably, particularly when it is associated with a heavier normal load. This is a consequence of the large tangential displacement the rubber undergoes in the contact area.

Hahn and Levinson[9], in 1974, gave a two dimensional linear elastic analysis for the quasistatic, frictionless indentation problem with the exact formulation. They assumed that the rubber-like layer is made of a Hookean material and its deformation is within the range of applicability of the linear theory. The problem is solved by using an Airy stress function and the solution is in terms of double infinite series, one of which converges slowly.

Batra[10], in 1980, approached the problem of a rubber covered roll, indented by a rigid cylinder, numerically by using the finite element method(FEM). He assumed that the material of the rubber-like layer is homogeneous and can be modeled as a Mooney-Rivlin material, as discussed in section 3.5. He treated his problem as a plane strain large deformation situation, and because of this Mooney-Rivlin material like characteristic of the rubber cover, and based on the experimental finding that the maximum strain commonly encountered in practice is probably much higher than what is usually thought to be the range of applicability of the linear theory, he considered his problem to be nonlinear. To solve his finite element model, he assumed the half width and a form of pressure profile at the contact area. The results obtained were in good agreement with the experimental results of Spengos. The only noticeable difference between the two results was explained as being due to the assumption of plane strain made in his work was not quite valid for Spengos' experimental set up, wherein a three dimensional state of strain existed.

In 1993, Diel, Stack and Benson[11] evaluated the axial variations in nip parameters such as contact pressure, contact area generated by deformation of the drums and the elastomeric covering for two general cases; an identical-hollow-drum design and a classic calendering design. Both cases included the effects of elastomeric coverings.

Comparison they made were between modeling the resolution axial variations in nip parameters by beam effects and shell effects for the identical-hollow-drum design. They found that the primary cause of axial variations in nip parameters was the axial variation in the drum's deflection. The shell models predicted much greater axial variation than the beam models due to localized shell effects. Also, at the end of the drum, the elastomer was not constrained and tended to behave softer. Therefore, near the free edge of the nip, edge effects became dominant in the thin elastomeric covering on the drums. Moreover, for the classic calendering problem, only the free edge effect of the thick elastomeric covering caused axial variations in nip parameters. They, also, found that decreasing the radius of the noncovered rigid roller increases both measures of speed ratio, i.e., ratio of speed of the undeformed covered roll and that of the deformed covered roll, and their axial variations.

Thus, to date, no nip roll in which an elastomeric covered roller contacts a rigid roller has been successfully analyzed without assumptions of contact width pressure distribution. There is no reference whatsoever regarding the solutions of contact problems between nip rollers and wound rolls.

CHAPTER III

CONTACT OF ELASTOMERIC COVERED ROLLERS WITH RIGID ROLLERS

If the indentation of the rubber covered roller in the nip is appreciably greater than the change in the thickness of the processed material, the presence of this material will have very little effect on the roller deformation. This allows webs transported through nip rollers to be treated as two cylindrical rollers in contact. As described in chapter 2, this type of problem is difficult to solve analytically since the pressure profile at the contact area and the contact width are unknown. And, due to instrumentation difficulties, it is not easy to obtain experimental results. Hertz's theory is applied well in linear elastic, small strain contact problems. Unfortunately, many web handling devices do not exhibit linear-elastic material behavior and often involve nonlinear deformation. So, numerical analysis can be considered as an appropriate method to solve this kind of problem. The finite element method, whose attributes are accuracy, flexibility and adaptability, is one of the most powerful tools. A FEM model of a rubber-covered roller has been developed using the finite element code MARC[12]. A new instrumentation, called Tekscan, is also used in experimental investigation of the contact pressure and contact area[13].

3.1 Experimental Setup

A schematic diagram of the system to be studied is shown in Fig. 3.1.

The main components of the experimental setup include a rigid nip roller, a rubber covered roller and two Bellofram air cylinders, each with a pressure gage.

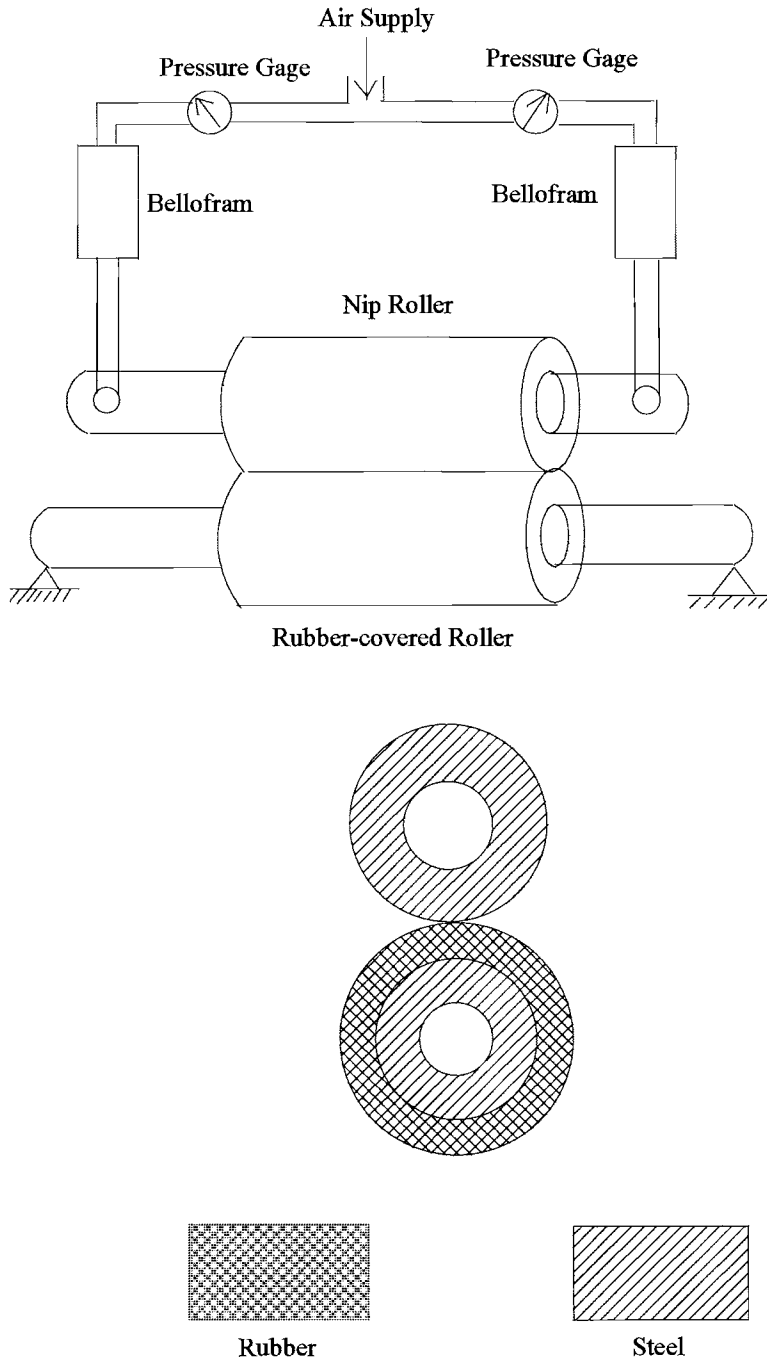


Fig.3.1 A Schematic Diagram of the System in Experiment

A load cell, connected with a digital strain indicator is used to calibrate the Belloframs. The result is seen in Fig. 3.2. We can see that the nip load varies linearly with the air pressure supplied to the Belloframs. From the curve fit equations, we can infer the nip load is based upon the supplied air pressure. The total nip load will include two Bellofram loads and the nip weight.

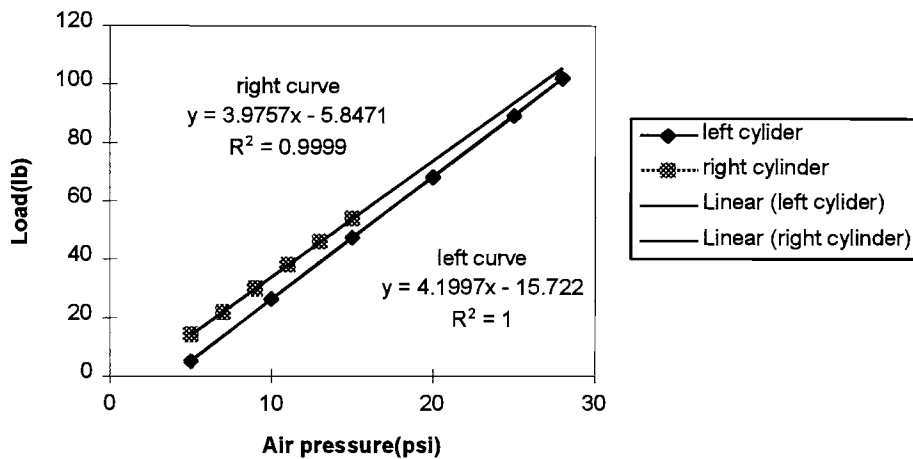


Fig.3.2 Nip Loads vs. Air Pressure Applied

3.2 Tekscan Measurement

The Tekscan sensor is a new kind of Force Sensing Resistor(FSR). It consists of an array of hundreds of force sensitive resistors and is only 4 thousandths of an inch thick. The sensor is connected with a computer through interface and software. An FSR is one of the devices commonly used in measuring pressure. It changes resistance when the force is applied on its surface. A good description of a FSR is given in reference[14]. It is very convenient to use but has slow dynamic response, which may influence the result. The Tekscan array sensor has the same dynamic response, so it is very important to use this sensor properly. After running several experiments, the

following recommendations can be made for using the Tekscan system. Sensor calibration should be performed prior to each measurement. When this research began, Tekscan was using a one point calibration routine. On a log-log plot, the resistance of a FSR is linear with pressure. The early Tekscan calibration software assumed that the slope of this line was constant and the line was located vertically on the log-log scale by a one-point calibration (i.e. the sensor was submitted to a known pressure and the data acquisition system read the change in voltage across the FSR sensors from which the resistance due to the calibration pressure could be inferred). The slope of the line is dependent on the quality control of the pressure sensitive inks used in the FSR. The overall resolution of the Tekscan sensors was 5% of the full scale pressure with one-point calibration. After pressure from 3M company and OSU, Tekscan began using a two point calibration routine which allowed the slope to be determined for each sensor. Make sure that the two points in pressure used in the two point calibration are within the load range of the experiment. While doing calibrations, leave the dead weight for a short certain time, like 20 seconds, on the surface of the sensor. Then, record the data after the same certain time while taking measurements.

Another important point is surrounding the sensor with the same material as that used in the experiment during calibration. In this experiment, the sensor will be inserted into the contact area between the nip and rubber-covered rollers. The rubber is soft material and experiences large deformations. If the sensor is calibrated on a flat and hard surface, it will have an error of one-third percent of integrated load in measurement. This becomes another contact problem. In these experiments, the Tekscan pressure sensors were calibrated by inserting them into a flat stack of material, which was of the same thickness and material properties as those materials to be tested, and subjected to known pressures.

3.3 Hertz's Theory

The first analysis of contact stress of two elastic bodies was made by Hertz[1].

His linear theory is satisfactory. He made the following assumptions:

- 1) the surfaces are continuous and non-conforming,
- 2) the strain is small. The dimensions of the contact area are small compared with the dimensions of the bodies and with the relative radius of curvature,
- 3) the contact bodies are considered homogenous and isotropic bodies,
- 4) the surfaces of contact bodies are frictionless,
- 5) the problem is a plane strain problem.

When two cylindrical rollers, (radius R_1 and R_2), with their axes both lying parallel, one pressed in contact by a force P per unit length, they make contact over a long strip of width $2a$ lying parallel to the cylinders' axes (see Fig. 3.3). Then, based on the above assumptions, through mathematical derivation, we have the following forms.

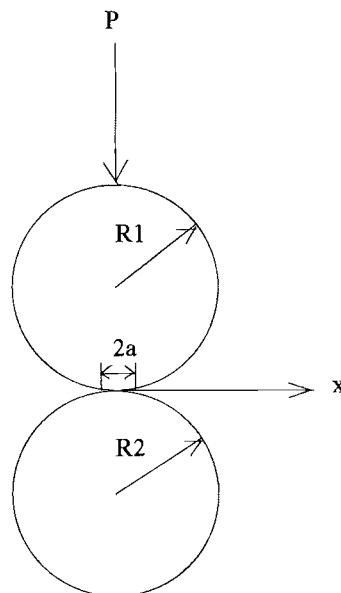


Fig. 3.3 Contact Rollers

Hertz assumed that the pressure distribution along x direction is:

$$p(x) = \frac{2P}{\pi a^2} (a^2 - x^2)^{1/2} = \frac{2P}{\pi a} \left(1 - \frac{x^2}{a^2}\right)^{1/2} \quad (3.1)$$

where x is the present distance measured from the center line of the nip ($-a \leq x \leq a$) and

p(x) is the pressure at point x.

The half of the contact width is :

$$a = \left(\frac{4 PR}{\pi E^*} \right)^{1/2} \quad (3.2)$$

where $\frac{1}{R} = \frac{1}{R_1} + \frac{1}{R_2}$

and $E^* = \left(\frac{1 - \nu_1^2}{E_1} + \frac{1 - \nu_2^2}{E_2} \right)^{-1}$

In our case, the nip is a comparatively rigid body, which has a much higher modulus of elasticity ($30 \cdot 10^6$ psi) than the rubbers (700 psi). So, we can assume $\frac{1 - \nu_1^2}{E_1} \approx 0$, when $E_1 \rightarrow \infty$.

That is :

$$E^* = \frac{E_2}{1 - \nu_2^2}$$

where E_2 is the rubber's Young's modulus and ν_2 is the rubber's Poisson's ratio

Therefore,

$$a = \frac{4 PR (1 - \nu_2^2)}{\pi E_2} \quad (3.3)$$

and the maximum pressure P_m is obtained at $x=0$, by Hertz was:

$$P_m = \frac{2 P}{\pi a} \quad (3.4)$$

In this experiment, a hard rubber covered roller with a durometer of 80 is used to verify the Hertz theory. The radius of the nip is 2 inches, and the rubber roller has the following properties:

Young's modulus: $E_2=707.64$ psi

Poisson's ratio: $\nu_2=0.45$

Radius: $R_2=2.72$ inches

The comparison of the results from Hertz and Tekscan is quite close and is shown in Fig.3.4. The maximum error of 14.4% was computed at 4.8 load level.

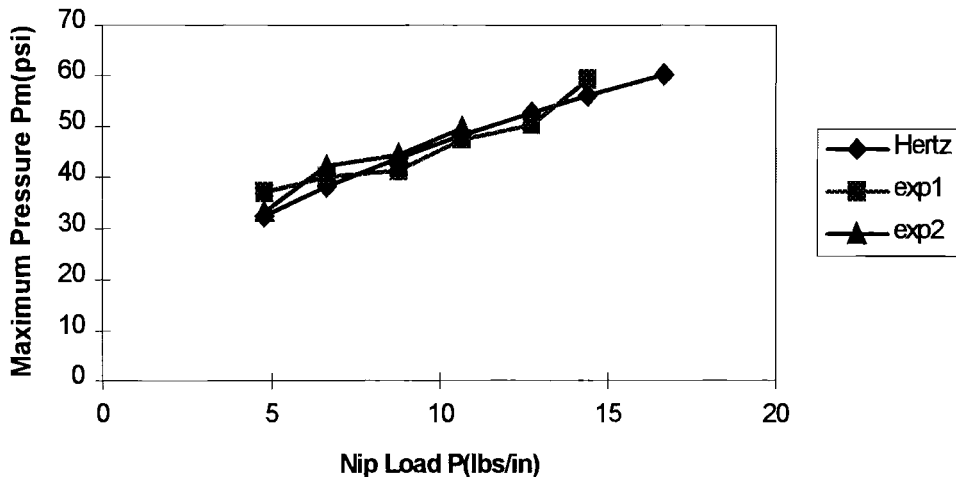


Fig. 3.4 Variation of Maximum Pressure with Nip Load as Predicted by Hertz and via Experiments

Because the contact area between the two rollers is small compared with the FSR density upon the Tekscan sensor, tests in which the contact width was studied as a function of nip load could not be performed with this material.

3.4 Finite Element Analysis

A 2-D plane strain FEM model was composed by using MARC, a powerful finite element package. The MARC system contains a series of integrated programs that facilitate analysis of engineering problems in the fields of structural mechanics, heat transfer, and electromagnetics. The computer code includes algorithms for large strain, linear or nonlinear material laws, and general contact between flexible and rigid bodies.

In MARC, the contact problem is considered to be a nonlinear problem. There are three sources of nonlinearity: material, geometric and nonlinear boundary conditions. Contact leads to nonlinear boundary conditions. A problem is nonlinear if the force-displacement relationship depends on the current state (i.e., current displacement, force, and stress-strain relations).

$$P=K(P,u)u$$

where P is a generalized force vector, K is the stiffness matrix and u is a generalized displacement vector. Nonlinear analysis is usually more complex and expensive than linear analysis. Also, a nonlinear problem can never be formulated as a set of linear equations. In general, the solutions of nonlinear problems always require incremental solution schemes and sometimes require iteration (or recycles) within each load/time increment to ensure that equilibrium is satisfied at the end of each step.

$$[K] [du] = [dp]$$

All contact problems require a time step and the number of time steps must be enough to insure a good result. The procedure is often very slow and tedious.

The Herrmann incompressible plane strain element is used here since Poisson's ratio of rubber used in the experiment is nearly equal to one-half. The Herrmann formulation allows the correct treatment of incompressible behavior without the

numerical difficulties associated with conventional displacement formulation elements. In particular, conventional elements should not be used in plane strain, axisymmetric or 3-D continuum analysis if Poisson's ratio is close to 0.5. MARC element 80 is used for this cylinder model. The element is a 5-node isoparametric, quadrilateral plane strain element. The fifth node is the extra pressure node, meaning it only has a pressure degree of freedom which is not shared with other elements. This extra node doesn't require the usual spatial coordinates to be defined.

If the pressure distribution is found, then the load pressing the rolls together can be calculated as :

$$P = 2 \int_0^a p(x) dx \quad (3.5)$$

In practice, the load P is specified. Contact width $2a$ and pressure $p(x)$ at the contact surface are unknown and are to be determined as part of the solution. One of the methods to solve the problem is to assume the half nip width and the pressure distribution $p(x)$, and find the load pressing the two rollers. One must iterate on the pressure distribution to arrive at the actual distribution. Another approach is to prescribe the indentation between the two rollers and to compute the necessary load. In the MARC program, all contact problems are solved by assuming an indentation.

Theoretically, for a symmetrical plane strain model, 180 degrees in the hoop direction should be modeled. However, for the contact solutions presented here, the deformation is localized near the contact area. And, in order to decrease the computational costs and computer memory space limit, 90 degrees is modeled. The mesh is finer in the contact area. This provides a more accurate measure of nip width and other nip parameters. The mesh plot is shown in Fig 3.5.

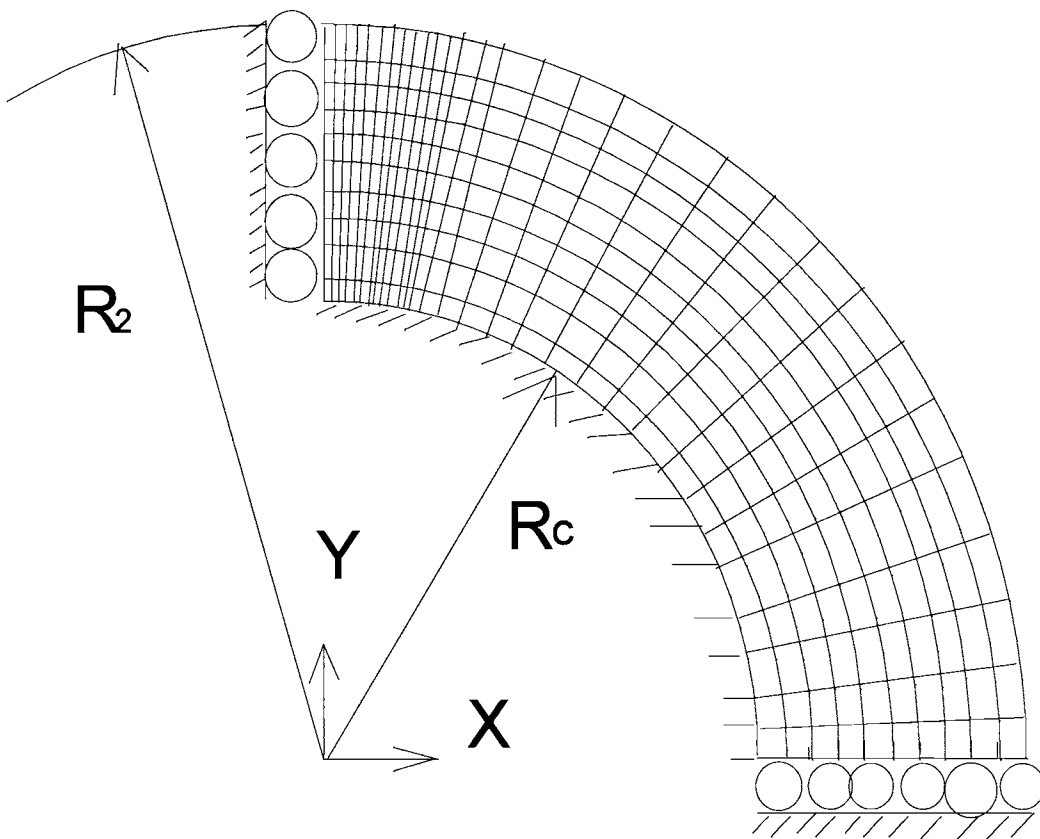


Fig 3.5 Finite Element Grid

3.5 Comparison of Results

A soft rubber covered roller used in the FEM model and the experiment has the following properties:

Radius: $R_2=2.053$ inches

Young's modulus: $E_2=240$ psi

Poisson's ratio: $\nu_2=0.45$

The radius of the steel core (R_c) is 1.47 inches and the radius of the nip roller is 2 inches.

In the FEM analysis, the following assumptions are made for the ease of computation:

- 1) the rubber covered material is assumed to be linear and isotropic,
- 2) the rollers are stationary and the problem is static,
- 3) the contact surface between the rollers is frictionless.

Fig. 3.6 shows the variation of nip load with contact width. Results from the finite element solution are compared with those from Hertz's theory and experimental data from the Tekscan sensor.

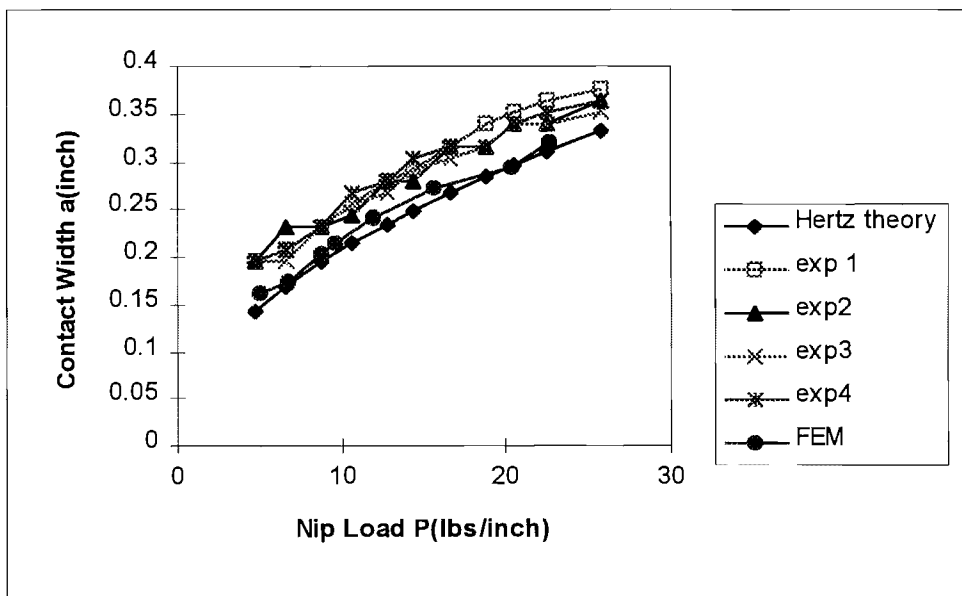


Fig 3.6 Variation of Contact Width with Nip Load

The FEM result is close to the Hertz theory, which is calculated by Eq.3.3.

Measurements from the Tekscan sensor are higher than the Hertzian result. The reason is that this rubber is soft and has more deformation than the hard one.

The relation between the nip load and the maximum pressure is shown in

Fig. 3.7. The Hertzian calculation is made using Eq.3.4. The three results agree well.

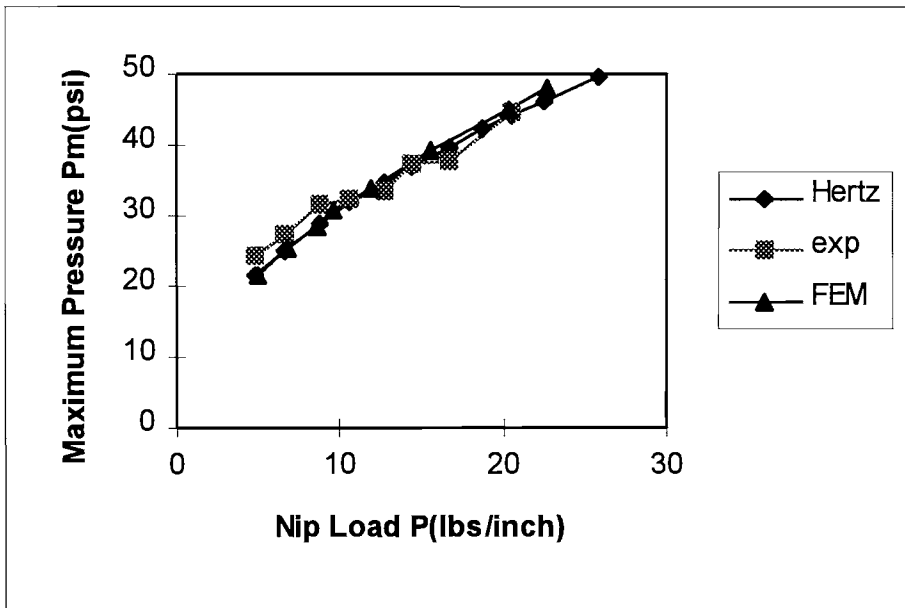


Fig. 3.7 Variation of Maximum Pressure with Nip Load

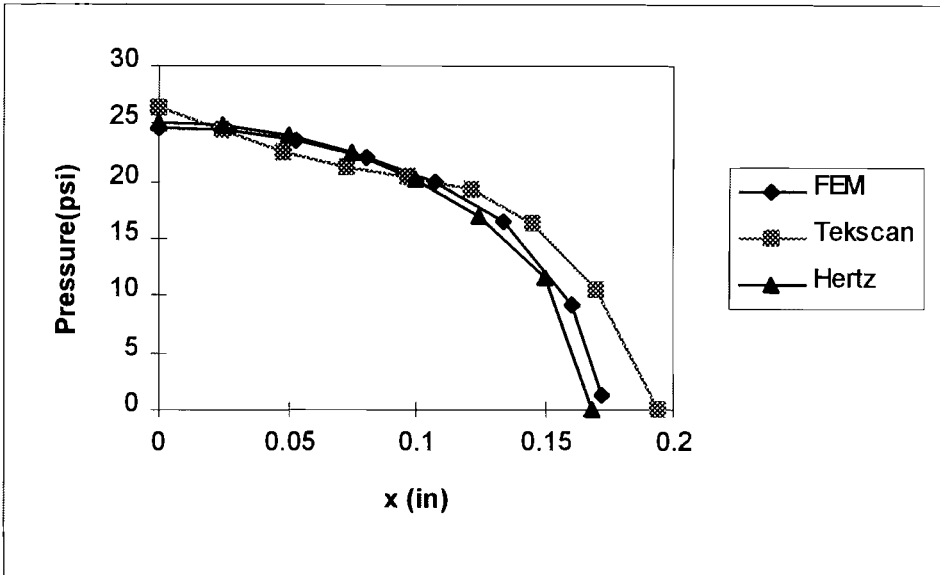


Fig 3.8 Pressure Distribution on Contact Surface -- Nip Load = 6.6 lbs/in

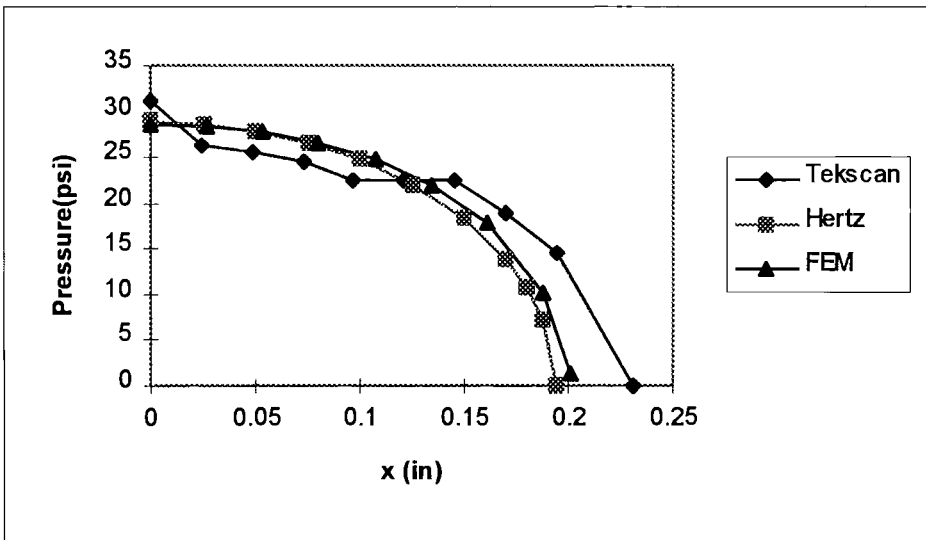


Fig. 3.9 Pressure Distribution on Contact Surface -- Nip Load = 8.8 lbs/in

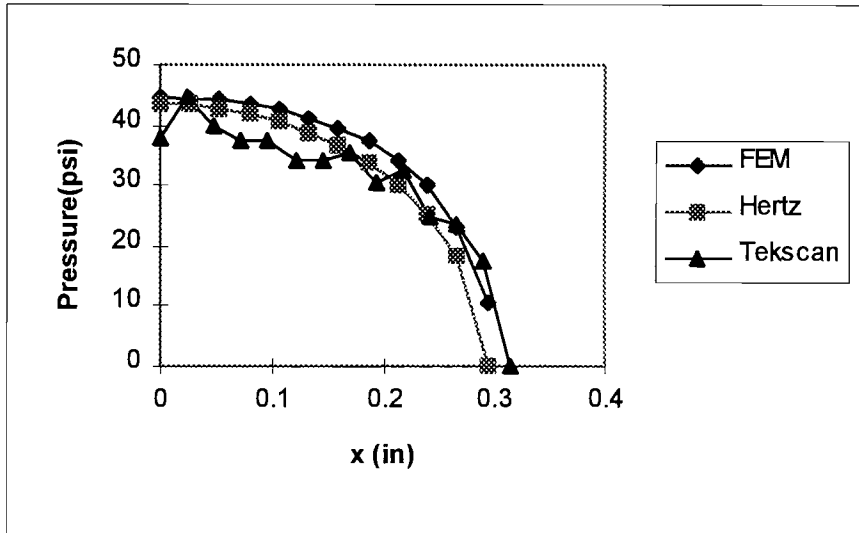


Fig. 3.10 Pressure Distribution on Contact Surface -- Nip Load = 20 lbs/in

Figs. 3.8, 3.9 and 3.10 show the pressure distribution along the contact area. The FEM and Hertz produce similar results. All methods agree well from $x=0.2$ to 0.25 in Fig. 3.10, and their curve shapes are similar in the area close to the end of the contact width in Figs. 3.8 and 3.9. However, in the maximum pressure area, measurement from Tekscan is different from the two analytical methods. From Eq. 3.5 we can see that in the plot of pressure profile vs. half contact width, the area beneath each curve should be about half of the total nip load. Spreadsheet software can be used to do approximate calculations of area by using the data in Figs 3.8 , 3.9 and 3.10. The areas beneath the three curves are very close to half nip load, except the value from Tekscan is larger in these figures (see Table 1).

	Half nip load (lbs/inch)	Area beneath Hertz curve	Area beneath FEM curve	Area beneath Tekscan curve
Fig. 3.8	3.3	3.27	3.36	3.59
Fig. 3.9	4.4	4.38	4.55	4.78
Fig. 3.10	10.0	9.96	10.89	9.96

Table 1 Comparison of Area Beneath Three Curves

3.6 Mooney-Rivlin Materials

As described in Chapter 2, Batra analyzed the indentation of an elastomer layer covered roller by a rigid body. He assumed the rubberlike material to be homegenous Mooney-Rivlin material, a kind of elastromeric and incompressible material.

Elastomeric materials are elastic in the classical sense. Upon unloading, the stress-strain curve is retraced and there is no permament deformation. Elastomeric materials are initially isotropic. An elastomer is a polymer which shows nonlinear elastic stress-strain behavior. One of the two elastomer modes used in MARC has the following strain energy function:

$$W=C_{10}(I_1-3)+C_{01}(I_2-3)+C_{11}(I_1-3)(I_2-3)+C_{20}(I_1-3)^2+C_{30}(I_1-3)^3$$

where

W is the strain energy function,

C_{10} , C_{01} , C_{11} , C_{20} , C_{30} are material constants obtained from experimental data,

and I_1 , I_2 are the first and second invariants of the elastic strain.

Mooney-Rivlin materials have a reduced form of the above strain energy function

$$W = C_{10}(I_1-3) + C_{01}(I_2-3) .$$

For Mooney-Rivlin materials, C_{10} and C_{01} are the only two material constants. These values can only be obtained from experimentation. The force and deformation for a uniaxial test specimen may be related as

$$P = 2 A_0 \left(1 - \frac{1}{\lambda_1^3}\right) (\lambda_1 C_{10} + C_{01})$$

where

P is the force of the specimen,

A_0 is the original area of the specimen, and

λ_1 is the uniaxial stretch ratio.

This equation and the associated test provide a simple way to determine the Mooney-Rivlin constants. The Mooney-Rivlin constitutive equation is applicable if the plot of

$$\frac{P}{2 A_0 \left(1 - \frac{1}{\lambda_1^3}\right)}$$

versus the stretch ratio results in an approximately straight line. See the Fig. 3.11.

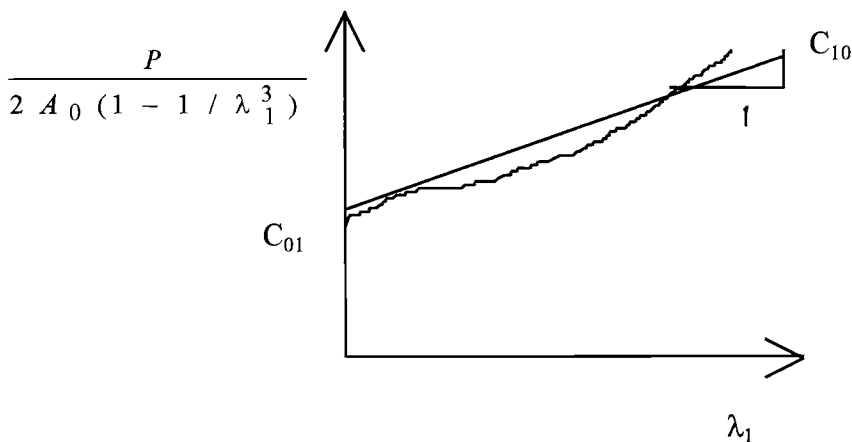


Fig. 3.11 Correlation With A Straight Line Using the Mooney-Rivlin Constitutive Equation

If only the Young's modulus E is supplied, and full uniaxial data are not available, then

$$C_{01} \cong 0.25 C_{10}$$

is a reasonable assumption. The constants then follow from the relation:

$$6 (C_{10} + C_{01}) \cong E$$

Mooney-Rivlin materials are defined in the MARC material library. Here a material model is made to compare the result with Batra's work. The rollers used in this model correspond to run number 30 of Spengos. That is, $R_1=7.62$ cm, $R_2=6.07$ cm and $R_c=4.72$ cm. The nip load is 92 lbs/inch, and the rubber modulus is 250 psi. The results are shown in Fig. 3.12. We can see the maximum pressure and contact width from the FEM analysis is close to Spengos' work. The pressure distribution in the contact area has light difference with Spengos' measurement since the maximum pressures are different. Batra's work, in reference [10], has good agreement with Spengos. However, he only showed the relation between pressure/peak value and x/a , which couldn't show how the pressure is distributed. This relation is shown in Fig. 3.13. The result from MARC is quite close to Spengos' and Batra's works. The maximum pressure and contact width calculated by Hertz's formula are 86 psi and 0.68 inch, which vary from the values measured by Spengos. Therefore, Hertz's theory does not provide accurate results for this kind of material. Although the material Spengos used has almost the same modulus of elasticity as that used in section 3.5, the materials behave differently because of the different loads. The maximum load used in section 3.5 is only 25 lb/in, but Spengos used 92 lb/in. So, when the load is small, the soft rubber might still behave linearly. But, when the load is large, the soft rubber behaves nonlinearly.

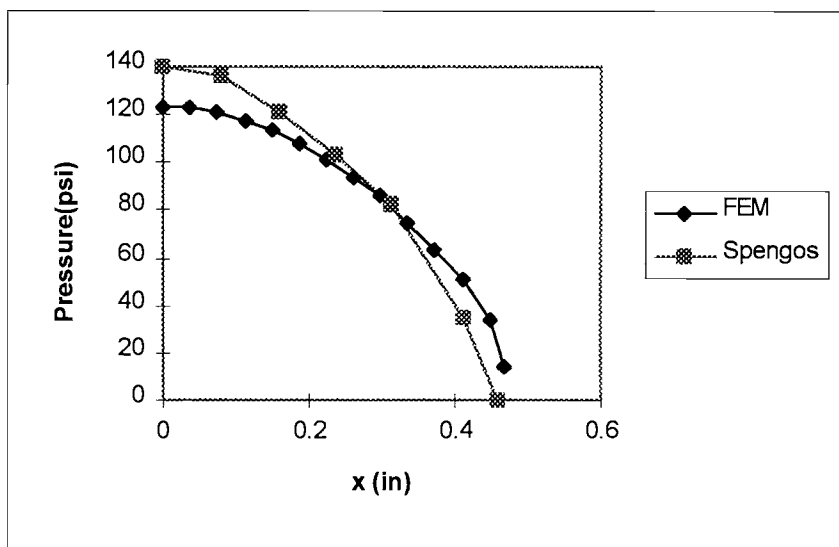


Figure 3.12 Pressure Distribution on Contact Surface

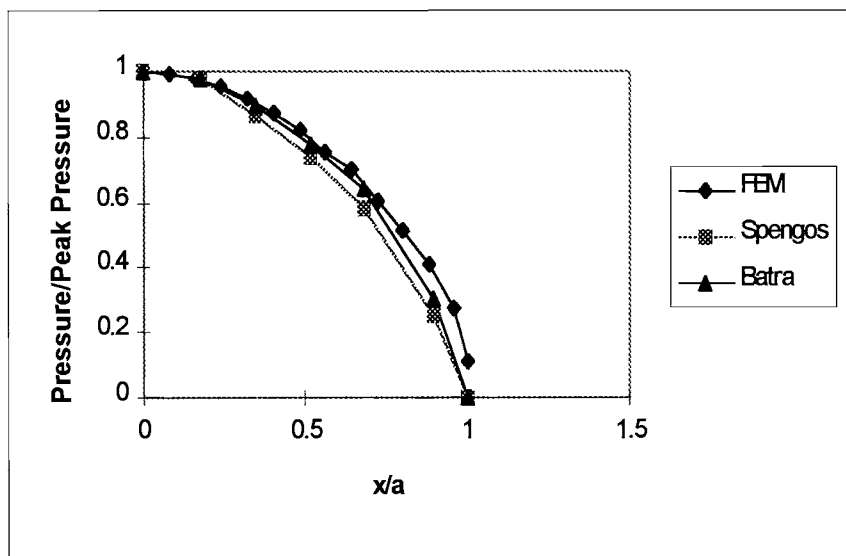


Fig. 3.13 Comparison of Result from FEM, Spengos and Batra

CHAPTER IV

CONTACT OF A RIGID ROLL WITH A WINDING ROLL

The prediction of stresses in the wound rolls has received much attention during the past decade. There are a number of wound roll models that predict stress distribution for center winding, the most rigorous of which are made by Hakiel[15], Pfeiffer[16], and Willett & Poesch[17]. One feature of these three models is that they allow the radial modulus, E_r , of a wound roll to be a function of radial stress. Laboratory experiments have demonstrated that the radial modulus is indeed a function of pressure. As described in Chapter 1, the nip roller affects the Wound-On-Tension, and further, affects the residual stresses in the wound roll. Since the paper roll is considered as orthotropic, nonlinear material, the classical linear theory and general nonlinear solution are not suitable for the contact problem of a nip roll with a winding roll. The material properties have to be obtained from experiments. Hakiel's model is the one most often used in web handling and is the one used in this study. A 2-D nonlinear FEM model, with E_r as a function of pressure, has been configured in this chapter. An experimental investigation is made using the Tekscan sensor.

4.1 Experimental Setup

The experiments were performed using the 3M splicer winder. Figure 4.1 shows the layout of the center winding with the nip roller on this machine. Center winding is

implemented by driving the roll core using a motor. The nip load is applied by attaching dead weights to a pulley system which is attached to the pivot bar. The tension sensor was calibrated by hanging a dead weight at the beginning of each test.

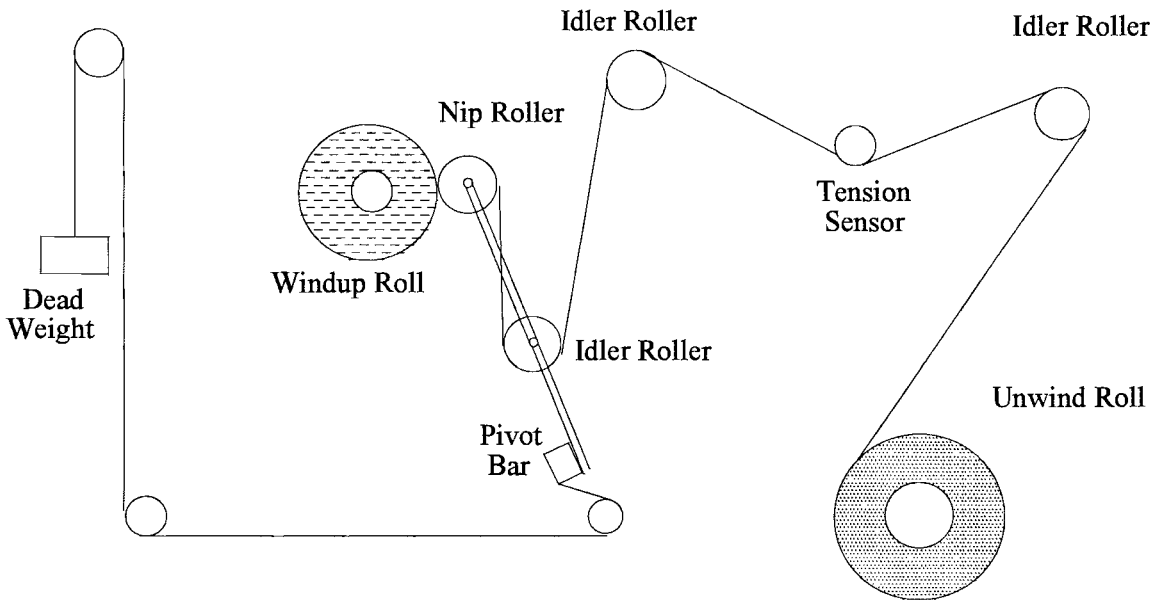


Fig. 4.1 Layout of Center Winding with Nip Roller on 3M Splicer Winder

4.2 Material Properties of Bond Paper

Bond paper was used in this study. The properties of bond paper, which include web thickness, Kinetic coefficient of friction between sheets of paper, radial modulus E_r and tangential modulus E_θ , etc., were determined.

There are a couple of ways to measure the web thickness. One is to use the Schaevitz LVDT noncontact caliper measurement gage. As a piece of bond paper moves from point to point under the air sensor, the meter will show the thickness. The average value of the thickness at 10 to 20 randomly selected points is used as the bond paper

thickness. Another way to determinate web thickness is to use a caliper to apply between 7 and 9 psi on a stack of paper which contains about twenty sheets[18]. The thickness of the stack divided by 20 is the bond paper thickness.

The friction coefficient was measured by a device[19] which consists of a motor, strain gage, gage indicator, computer data acquisition system, carriage and plate. Web sheets were stuck to the carriage and plate by tape. A dead weight of 2 lbs was put on top of the carriage. As the carriage moved, the data acquisition system processed the data and gave the friction coefficient.

The test in which E_r was measured was conducted using the Instron 8502 servo controlled load frame. In the experiment, a 1" thick stack of 6"x6" paper was used. The ramp speed was set very slow so that rate effects due to the expulsion of entrained air were minimized. The data acquisition was done using a GPIB interface and the load and stack displacement were stored on a data file which can be processed by spreadsheet software. The load and displacement data were used in a spreadsheet in calculations of stress and strain. The slope of the stress/strain data was then evaluated at various stresses which produced a table of E_r values at various stresses or equivalently, pressures. Then the mathematical representation of the radial modulus, E_r , was determined using a 3rd order polynomial curve fit in pressure.

The measurement of E_θ was performed using an Instron 4202 loading frame and a 1 inch wide by 10 inches long strip of bond paper cut along the tangential direction of the roll. The ends of paper strip were gripped by two clamps and then one end was pulled. The clamps should be chosen properly and the ends of the strip should be clamped correctly to ensure the strip is subjected only to uniform tensile stress. Otherwise, the measured tangential modulus would be less than the real value. The data acquisition for E_t was done using the Labtech notebook, a commercial data acquisition software package, which was used to collect the raw data for the E_r calculation as well.

From the tests described above, the parameters of bond paper are:

Thickness: $h = 2.6$ mil

Kinetic coefficient of friction between sheets of paper: $\mu = 0.255$

Radial modulus: $E_r = 50.38 * p - 0.321 * p^2 + 0.001 * p^3$ psi

Tangential modulus: $E_\theta = 510,910$ psi

4.3 Pull Tab Calibration

A pull tab, which consists of a brass shim stock and stainless steel feeler gauge, is an effective tool to measure the wound roll radial stress. Calibration of the pull tabs is very important to ensure accurate results. The test used a stack of bond paper 6"x6", with the same thickness as the paper to be wound. The core's radius is 1.7 inches and the outside radius of the paper roll is 5.1 inches. Therefore, the thickness of the bond paper stack is 3.4 inches. The stack, with a pull tab inserted, is put on an Instron 8502 and is compressed at various loads to produce various calibration pressures.

A force gage is used to pull the tab and measure the values corresponding to different pressures. Figure 4.2 shows the calibration curve of one of the 10 pull tabs used in these experiments.

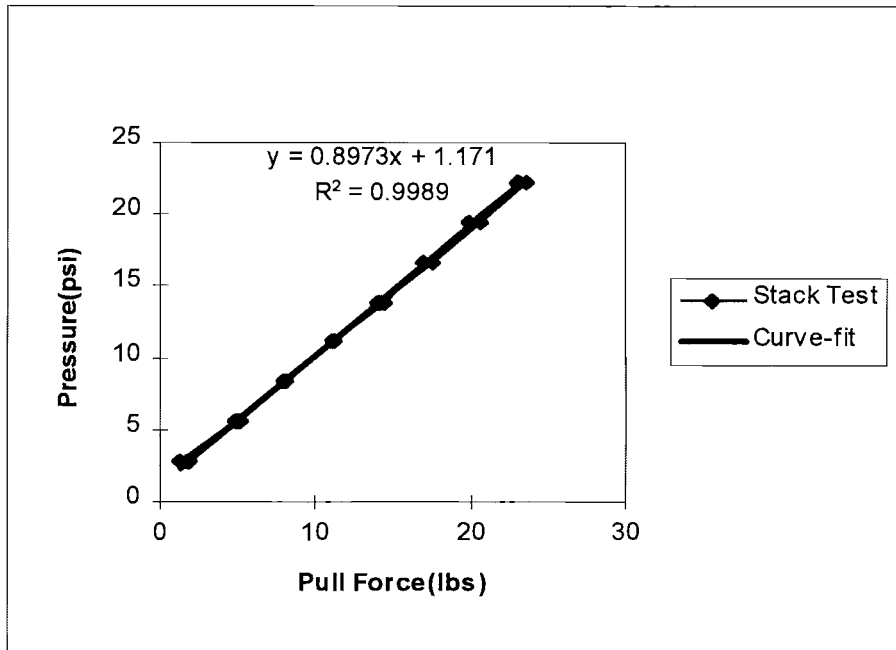


Fig. 4.2 Pull Tab Calibration

The calibration was done according to Cai's [19] recommendation. He suggests that only one pull tab be inserted in a stack in each calibration test. The tab's radial position in the paper stack will be the same as the position of the pull tab in the winding roll. The tab should be placed at the bottom position in the web stack, when the tab is going to measure the wound roll stress close to the core.

4.4 Hakiel's Model

In 1987, Hakiel[15] developed a model to predict the wound roll stress based upon the theory of elasticity. In his model, he made several assumptions:

- 1). the winding roll is treated as a geometrically perfect cylinder,
- 2). the roll is an orthotropic cylinder which has a linear elastic modulus in the circumferential direction and a nonlinear elastic modulus in the radial direction,

3). the stresses in the wound roll are assumed to be functions of the radius, but not of the axial or circumferential position,

4). the plane stress condition is assumed.

By solving a set of algebraic equations, which resulted from the recursive application of a second order ordinary differential equation with non constant coefficients and two boundary conditions, the distribution of radial pressure and circumferential stress can be obtained. In order to solve a set of algebraic equations, the finite difference method and the Gaussian elimination method are applied in this model. Using the finite difference method, the derivative terms in the ordinary differential equation are simplified by central difference approximations. The program, called Winder, which was developed at the Web Handling Research Center (WHRC) and contains Hakiel's model, is used to compare the pressure from Hakiel's model with the results from the pull tab experiment. The comparison is shown in Figure 4.3. The results match well. This stress status is used as the initial status of the FEM model.

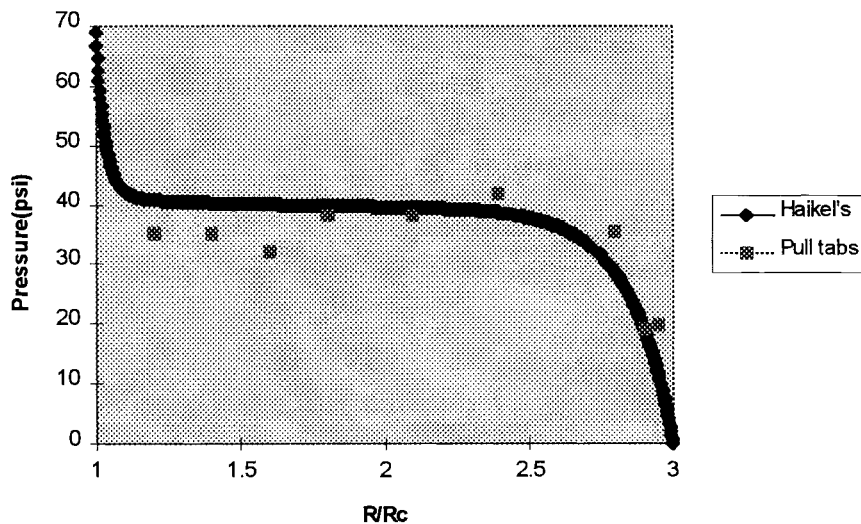


Fig. 4.3 Interlayer Pressures at Center Winding with 500 psi Tension and 4pli Nip Load

$$\begin{aligned}\frac{\partial r}{\partial x} &= \cos\theta, & \frac{\partial r}{\partial y} &= \sin\theta, & \frac{\partial r}{\partial z} &= 0, \\ \frac{\partial \theta}{\partial x} &= -\sin\theta, & \frac{\partial \theta}{\partial y} &= \cos\theta, & \frac{\partial \theta}{\partial z} &= 0, \\ \frac{\partial z'}{\partial x} &= 0, & \frac{\partial z'}{\partial y} &= 0, & \frac{\partial z'}{\partial z} &= 1.\end{aligned}$$

where r is the radial direction and θ is the tangential direction.

Therefore, the transformation matrix is:

$$\begin{bmatrix} \cos\theta & \sin\theta & 0 \\ -\sin\theta & \cos\theta & 0 \\ 0 & 0 & 1 \end{bmatrix}$$

(3) Subroutine Anelas allows the user to define the anisotropic elastic law. In plane stress, the linear orthotropic constitutive equations in local coordinates are:

$$\begin{bmatrix} \varepsilon_r \\ \varepsilon_\theta \\ \gamma_{r\theta} \end{bmatrix} = \begin{bmatrix} 1/E_r & -\nu_{\theta r}/E_\theta & 0 \\ -\nu_{r\theta}/E_r & 1/E_\theta & 0 \\ 0 & 0 & 1/G_{r\theta} \end{bmatrix} \begin{bmatrix} \sigma_r \\ \sigma_\theta \\ \tau_{r\theta} \end{bmatrix}$$

The inverse form is the elastic law used in MARC, which is:

$$\begin{bmatrix} \sigma_r \\ \sigma_\theta \\ \tau_{r\theta} \end{bmatrix} = \begin{bmatrix} a_{11} & a_{12} & 0 \\ a_{12} & a_{22} & 0 \\ 0 & 0 & a_{66} \end{bmatrix} \begin{bmatrix} \varepsilon_r \\ \varepsilon_\theta \\ \gamma_{r\theta} \end{bmatrix}$$

where the a_{ij} , commonly termed the reduced stiffness coefficients, are given by:

$$\begin{aligned}a_{11} &= \frac{E_r}{1 - \nu_{r\theta}\nu_{\theta r}} & a_{22} &= \frac{E_\theta}{1 - \nu_{r\theta}\nu_{\theta r}} \\ a_{12} &= \frac{\nu_{\theta r}E_r}{1 - \nu_{r\theta}\nu_{\theta r}} & a_{66} &= G_{r\theta}\end{aligned}$$

where the shear modulus can be obtained from reference [21],

$$G_{r\theta} = \frac{(E_r * E_\theta)}{2 * (1 + (\nu_{r\theta} * \nu_{\theta r})^{1/2})}$$

From strain energy constraints:

$$\frac{\nu_{r\theta}}{E_r} = \frac{\nu_{\theta r}}{E_\theta}$$

In Hakiel's model, Poisson's ratio is defined as $\nu = \nu_{\theta r}$.

The material properties E_θ , E_r have already been shown in Section 4.2 and $\nu=0.01$.

As mentioned above, MARC only uses global constants, which have the form:

$$\begin{bmatrix} \sigma_x \\ \sigma_y \\ \tau_{xy} \end{bmatrix} = \begin{bmatrix} b_{11} & b_{12} & b_{16} \\ b_{12} & b_{22} & b_{26} \\ b_{16} & b_{26} & b_{66} \end{bmatrix} \begin{bmatrix} \varepsilon_x \\ \varepsilon_y \\ \tau_{xy} \end{bmatrix}$$

where the b_{ij} are related to the a_{ij} by the following equations[22] if c denotes $\cos\theta$ and s denotes $\sin\theta$:

$$\begin{bmatrix} b_{11} \\ b_{12} \\ b_{22} \\ b_{16} \\ b_{26} \\ b_{66} \end{bmatrix} = \begin{bmatrix} c^4 & 2c^2s^2 & s^4 & 4c^2s^2 \\ c^2s^2 & c^4 + s^4 & c^2s^2 & -4c^2s^2 \\ s^4 & 2c^2s^2 & c^4 & 4c^2s^2 \\ c^3s & -cs(c^2 - s^2) & -cs^3 & -2cs(c^2 - s^2) \\ cs^3 & cs(c^2 - s^2) & -c^3s & 2cs(c^2 - s^2) \\ c^2s^2 & -2c^2s^2 & c^2s^2 & (c^2 - s^2)^2 \end{bmatrix} * \begin{bmatrix} a_{11} \\ a_{12} \\ a_{22} \\ a_{66} \end{bmatrix}$$

Since the subroutine Orient has defined the transformation matrix between two coordinates, MARC will do the material properties transformation automatically.

(4) The value of $\cos\theta$ and $\sin\theta$ could be obtained either from the mesh dimensions or from subroutine Intcrd, which outputs coordinates of every element at each increment. Then, we have:

$$\cos\theta = \frac{x}{\sqrt{x^2 + y^2}}$$

$$\sin\theta = \frac{y}{\sqrt{x^2 + y^2}}$$

In order to see how the nip roller influences the outer regions of the paper roller, the elements of outerlayers of the roller surface in this model have the dimension as small as the web thickness which is 0.0026 inch. However, this value is so small that it can cause numerical difficulties for the program. Also, it will generate a mesh plot with a larger number of elements than is allowed by the computer memory. In order to overcome these disadvantages, a 45 degree model using only the outer 0.5 inch thickness of the paper roller was considered in this study, since the radial modulus of elasticity on the outside of this layer is 40 times less than that on the inside of the layer.

The results from the FEM analysis is compared with the Tekscan measurements and is shown in Fig. 4.4. Because the nip roller used in the experiment is misaligned, the pressures on one side of the center line of nip length is higher than the pressures on the other side, during the pressure measurement using Tekscan sensors. The pressures on both sides, which have the same distance to the center line of nip length, were compared in this figure. We can see that the result from the finite element solution is close to the average value of experimental data from the Tekscan sensors.

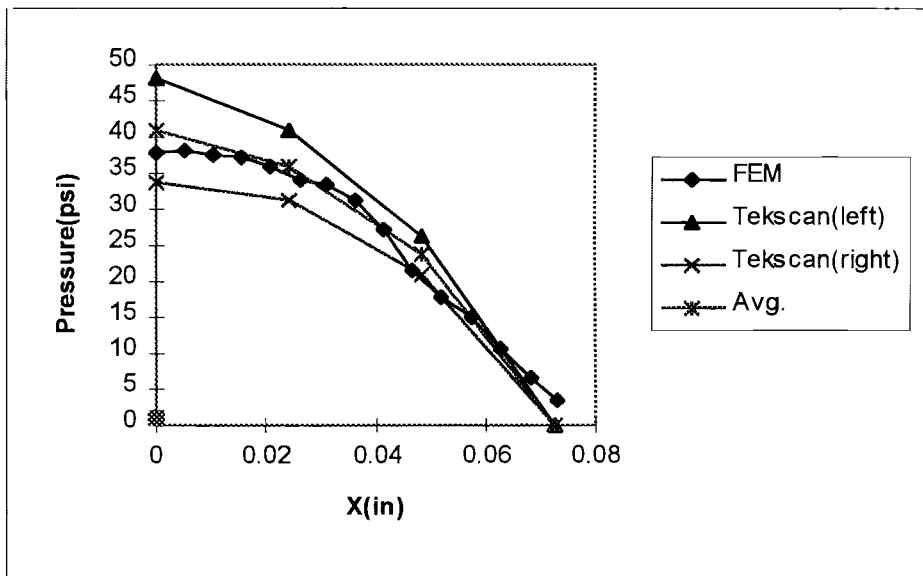


Fig. 4.4 Pressure Profile Along Half Contact Width with 4 pli Nip Load

CHAPTER V

CONCLUSIONS AND FUTURE WORK

5.1 Conclusions

A nonlinear contact problem of two cylinders is solved by using the finite element package MARC and the Tekscan sensor in this study. The analyses were done in two contact cases: a rubber-covered roller with a rigid roller and a winding paper roller with a rigid roller. From this study we can conclude :

1. Since hard rubber has a small deformation and satisfies Hertz's assumptions, his theory is applied well to the analysis of the contact of a hard rubber roller with a rigid roller.

2. For the soft rubber roller, when the load is small and the material behavior is linear, Hertz's theory still can be used. The only difference is that the real contact area is a little larger than Hertz assumed since soft rubber has more deformation. The maximum pressure produced by the nip loads in the experiments agrees with those based on Hertz's theory.

The results from finite element analysis, which considers the material as linear and isotropic, have good agreement with Hertz's theory, although the problem is only solved as a nonlinear boundary condition problem in the MARC. The pressure distributions away from center line are similar in the experiment, FEM analysis and Hertz's theory, but not in the area close to the center line.

3. If the rubber behaves nonlinearly under high load, namely, has a large strain like Mooney-Rivlin materials, FEM is adequate to analyze the problem. Hertz's theory can't be used in this case since his assumption that the material behaves linearly and has a small strain doesn't exist.

4. The pressure distribution at the contact area between a wound paper roller and a rigid roller, as determined by the FEM analysis, is close to the average value of the experimental investigation. This gives a good and effective way to analyze the contact problem with radial modulus as a function of pressure.

5.2 Future Work

Areas of future study should include:

(1) The deformation of the core and the indenting roller need to be considered for very thin rubber covers. The effect of the rubber layer thickness on the roller is not involved in this research. It may influence the relation between loading and deformation, as described in Chapter 2.

(2) Since axial variations in contact pressure and deformation can cause web wrinkling, and uneven material transfer, axial variations with radial modulus as a function of pressure need to be studied.

(3) The effect of friction at the contact surface between the roller, roller rotation and its dynamic effects should be studied.

REFERENCES

1. Hertz, H. "Über die Berührung fester elastischer Körper," Journal für die reine und Angewandte Mathematik, Vol. 92, 1881, pp.156-171.
2. Good, J. K. and Wu, Z. "The Internal Stresses in Wound Rolls with the Presence of a Nip Roller," Tappi Journal, 1992
3. Hannah, Margaret, "Contact Stress and Deformation in a Thin Elastic Layer," Quart. Journal of Mechanics and Applied Math, Vol.4,Pt.1,1951,pp.94-105.
4. Parish, G. J., "Measurement of the Pressure Distribution Between Roller in Contact," British Journal of Applied Physics, Vol.6, July 1955,pp.256-261
5. Parish, G. J., "Measurement of the Pressure Distribution Between Metal and Rubber Cover Roller," British Journal of Applied Physics, Vol.6, July 1955,pp.256-261
6. Parish, G. J., "calculation of the Behavior of Rubber-Covered pressure Rollers," British Journal of Applied Physics, Vol.12, July 1961,pp.333-336
7. Foreman, A. R., "Application of Rubber Covered Rolls to Pinch Rolls and Bridles," Iron and Steel Engineer Year Book, 1964,pp.646-656.
8. Spengos, A. C., "Experimental Investigation of Rolling Contact", Journal of Applied Mechanics, Vol. 32, December 1965,pp.859-865.
9. Hahn, H. T. and Levinson, M., "Indentation of An Elastic Layer(s) Bonded to a Rigid Cylinder- I. Quasistatic Case Without Friction", International Journal of Mechanical Science, Vol.16,pp489-502,1974.
10. Batra, R. C., "Rubber Covered Rolls-The nonlinear Elastic Problem", Journal of Applied Mechanics, Vol. 47, December 1965,pp.82-86.
11. Diehl T., Stack K.D., and Benson R.C., "A Study of 3-Dimensional on-Linear Nip Mechanics", Second International Conference on Web Handling, June, 1993
12. MARC Manul , Version 6.1, MARC Analysis Research Corporation, 1994.

13. Tekscan Operating Manul, Version 1.3, Tekscan, Inc., 1991.
14. Good, J. K. and Fikes M.W.R., "Predicting Internal Stresses in Centerwound Rolls with an Undriven Nip Roller," Tappi Journal, Vol, 74, no. 6, p101, 1991.
15. Hakiel, Z., "Nonlinear Model for Wound Roll Stress," Tappi Journal, Vol. 70, no. 5, pp113-117, May 1987.
16. Pfeiffer, J. D., "An Update of Pfeiffer's Roll-Winding Model," Tappi Journal, Vol. 70, no. 10, 1987.
17. Willett, M.S. and Poesch, W.L., "Determine the Stress Distributions in Wound Rolls of Magnetic Tape using a Nolinear Finite Difference Approach," Journal of Applied Mechanics, Vol. 55, pp. 365-371, 1988.
18. Ireland, G.H., "Paperboard on the Multi-vat Cylinder Machine," Chemical Publishing Company, Inc., 1968.
19. Ducotey, K.S., "Traction Between Webs and Rollers in Web Handling Applications," PhD. thesis, Oklahoma State University, May, 1993.
20. Cai Ning, "The effect of Nip Roll Compliancy Upon Center and Surface Winding", MS. Thesis, Oklahoma State University, December, 1992.
21. Baum G.A., Brennan D.C. and Habeger C.C., "Orthotropic Elastic Constants of Paper", Tappi, August, Vol. 64, No. 8, 1981.
22. Lekhnitskii, S.G., Anisotropic Plates, New York, McGraw-Hill, 1968.

VITA

Chunbao Xu

Candidate for the Degree of

Master of Science

Thesis: NIP ROLLER INDUCED CONTACT STRESSES

Major Field: Mechanical Engineering

Biographical:

Personal Data: Born in Fujian, P.R.China, April 17, 1968, the son of Shouren Xu and Fengchuan Zhu.

Education: Graduated from No. 3 Fuzhou Middle School, Fuzhou, Fijian, P.R.China, in July 1984; received Bachelor of Science Degree from Beijing University, Beijing, P.R.China, in July, 1988. Completed the requirements for the Master of Science degree with a major in Mechanical Engineering at Oklahoma State University in May, 1995.

Experience: Assistance administration in Natural Science Division of Beijing University; research assistant, Web Handling Research Center, School of Mechanical and Aerospace Engineering, Oklahoma State University, June, 1993, to December, 1994.